Fabrication and mechanical properties of porous titanium and its alloys for implant application

Wang, Jianfeng; Liu, Mark

Fabrication and Mechanical Properties of Porous Titanium and Its Alloys for implant application

J.F. Wang* and X.Y. Liu

Integrated Manufacturing Technologies Institute

National Research Council Canada

800 Collip Circle, London

ON N6G 4X8

Canada

*** Corresponding author**

Integrated Manufacturing Technologies Institute, National Research Council Canada, 800 Collip Circle, London, ON N6G 4X8, Canada

Tel: +1-519-4307094

Fax: +1-519-4307064

Email: jianfeng.wang@nrc.gc.ca

Abstract

Porous titanium and its alloys are attractive for orthopedic/dental implant applications because of their good biocompatibility and tailorable mechanical properties. This paper reviews recent advances in the development of porous titanium materials, including fabrication techniques for metal foams, powder-metallurgy methods for producing porous titanium structures, mechanical properties, and modeling of elastic behaviors by analytical methods. For orthopedic implant applications, porous titanium materials with Young's modulus close to that of cortical and cancellous bones can be fabricated by the adjustment of porosity and processing parameters. However, the overall mechanical performance of the porous titanium is not yet fully satisfactory for most load-bearing implants and further improvements in mechanical properties are needed.

Keywords: Porous titanium materials, Manufacture, Mechanical properties, Implants, Modeling

Introduction

Since titanium was commercially successful in 1948 [1], its excellent biocompatibility combined with high strength-to-weight ratio and high corrosion resistance has rendered titanium and its alloys (referred to collectively as titanium alloys hereafter) the most popular metallic biomaterials today. The potential of titanium alloys as surgical implant materials were mentioned as early as in 1951 [2], and the early uses of titanium alloys for implant applications were reported in the 1960s [3-5]. The use of titanium alloys as biomaterials has been growing steadily since the mid-1970s, and the trend is expected to continue into the future.

Numerous studies have been performed on the properties of titanium alloys in light of medical implant applications. In general, titanium alloys display (1) excellent biocompatibility (high chemical stability in the human body environment and low rates of metal ion release, no adverse cell or tissue reactions), (2) excellent corrosion resistance due to the stable passive surface oxides, and (3) good mechanical properties which allow load-bearing applications in dentistry and orthopedic implants. As shown in Table 1 [6], the relatively low young's modulus of titanium alloys, as compared to stainless steel, Co-Cr-Mo alloys, alumina and zirconia, makes titanium alloys a preferred choice for reducing the stress shielding effect and promoting load transfer to the bone. However, titanium alloys are more susceptible to wear and fretting than steel and cobalt chromium alloys [7]. The inadequate wear-resistance prevents titanium alloys from being used in applications where severe wear is expected. For the most part, titanium is not articulated against other materials or itself, but is used for components of modular construction. For

example, titanium femoral stem is used in combination with a cobalt-chromium or a ceramic ball (femoral head) articulating against a ultra high molecular weight polyethylene (UHMWPE) liner in a total hip replacement.

Porous titanium alloys are attractive for medical implant applications for two major considerations. The first one is that the porous surface promotes fixation of implants to the host tissue. The other is the tailorable elastic modulus of the porous materials that can be controlled to match that of natural bones. Reliably anchoring implants to host tissues is a key requirement for successful long-term performance of implants. Traditionally, polymethylmethacrylate (PMMA) based cement is used to provide immediate fixation between the implant and bone, which provides a fairly good long-term fixation. This type of procedures, however, is not suitable for young (<50 years) active patients where more stable fixation and allowance for bone growth are needed. Furthermore, problems of cell necrosis from the exothermic reaction of the cement while gelling, cement failure, or monomer release and loss of endosteum bone are still a concern with the cement fixation method [8,9]. Cementless fixation, on the other hand, achieve fixation primarily by biological means whereby press-fit insertion is followed by bone growth into a porous surface. Intimate contact between the porous surface and the surrounding bone and temporary immobilization are the prerequisites for the occurrence of bone ingrowth. Although some degree of micromotion of the implant is inevitable, it was revealed that the tolerated micromotion threshold is between 50 to 150 μm depending on surface state and implant design [10-11], making cementless fixation a feasible and generally accepted practice nowadays.

A number of techniques have been employed to modify the surfaces of implants for enhanced cementless fixation. Machined macroscopic anchorage elements, such as threads, vents, fins, grooves and serrations (in millimeter) or microscopic surface features (in submicron or micron range) are probably the earliest methods used for implant surface modifications. Microscopic surface modifications can be realized by removal of the material from an implant surface through grit blasting [12, 13], chemical treatment [14,15], addition of material to a substrate surface through plasma spraying [16], or sintering of particles onto the surface [17-19]. It has been proved that the three-dimensional nature of the open-pored structure is particularly suitable for implant fixation by tissue ingrowth [20-22] and the pore size must be in the range of 100 to 500 μm [23-26].

Another important concern regarding the durability of the implant is the biomechanical mismatch resulting from the difference in the elastic modulus of natural bone and the implant materials[27, 28], which leads to bone resorption and loosening of the joint [29-33]. This phenomenon, termed "stress-shielding induced bone resorption" is one of the main factors necessitating revision surgery. Any reduction in the stiffness of the implant, for example, through substitution of present orthopaedic alloys with newer, lower modulus materials, is expected to enhance stress redistribution to the adjacent bone tissues, therefore minimizing stress shielding and consequently prolonging device lifetime. The concern related to stress-shielding has stimulated considerable amount of research in the development of new materials with bone-matching modulus, such as

polymer based composites [34-41] and metastable β-Titanium alloys [27, 42-43], for the fabrication of permanent implants. A promising approach to reduce the elastic modulus is to use a porous structure, where the elastic modulus can be tailored by controlling the density/porosity of the porous body [44].

The combination of excellent biocompatibility with the tailorable mechanical properties and desired pore structure that enhances tissue ingrowth, makes porous titanium and its alloys attractive materials for advanced medical implant applications. This paper reviews the advances in the development of porous titanium alloys for orthopedic/dental implant applications. The topics include: the fabrication techniques to obtain the porous structure for titanium and its alloys, the mechanical properties of the porous titanium and its alloys, the predication of mechanical behaviours by the analytical methods, and the application of finite element analysis (FEA)

1. Fabrications of porous structure

A large variety of techniques have been developed for the fabrication of porous metal structures, involving liquid state processing, powder metallurgy (P/M), electro-deposition and vapour deposition approaches. Davies et al. [45] were the first to systematically classify the methods for producing porous metals, and later Ashby et al. [44] and Banhart [46] comprehensively summarized these methods in more detail.

The forming of porous metals using liquid state processing involves melting the metal, adding ingredients (such as SiC, Al_2O_3, Ca, or MgO.) to control viscosity of the melt as necessary, and injecting gas (air, nitrogen, or argon) into the melt using a rotating impeller [47-54], or adding a foaming agent (TiH_2, ZrH_2 or MgH_2) to the melt instead of blowing gas [55-60]. Some liquid metals form a eutectic system with hydrogen. By melting these metals in a high pressure hydrogen atmosphere, the melt is charged with hydrogen, as the melt cools, bubbles of hydrogen are released producing voids [61-70]. Another liquid processing technique, called powder compact melting, is realized by mixing and compacting metal/alloy powders with foaming agent powders followed by decomposition of the foaming agent in the molten state. The released gas forces the compacted precursors to expand to form a highly porous structure [71-74]. Casting a liquid metal around space holder materials or polymer foam is another approach to produce metal foams. Subsequent removal of the space holder leaves a porous structure [75-82]. An example of such an approach is the use of polymer foam and a soluble ceramic as the transient materials. The polymer foam is first filled with the slurry of the soluble ceramic. After drying, the polymer is removed by heat treatment and a molten metal is cast into the resulting ceramic structure with open pores. A metallic porous structure that exactly replicates the shape of the original polymer foam can be obtained by the removal of the soluble ceramic [83-84].

The techniques based on melting are suitable mainly for materials with relatively low melting temperature and reactivity, such as aluminum, magnesium and their alloys. They are, however, not suitable for producing porous titanium because of the very high

reactivity and high melting point of Ti (1670°C). Instead of the molten metal approach, P/M routes are generally employed for producing porous Ti. The P/M routes also allow microstructure refinement through the control of powder sizes, compaction and sintering parameters, thereby allowing control of mechanical properties. According to the pore formation mechanism, P/M routes for producing porous titanium can be divided into four categories: (1) sintering of Ti powders and fibers, (2) using a space holder, (3) employing pore-forming agents, (4) entrapped gas expansion.

1.1 Sintering of Ti powders and wires

Sintering packed powders or fibers is the easiest way to obtain porous metals and is a well established production route in P/M industry. Sintered titanium and Ti-6Al-4V porous body with different porosity characteristics can be achieved by varying initial compaction parameters and sintering conditions. Loose Ti-6Al-4V powders were sintered by Cirincione et al. [85] at 1000 °C for sintering time between 0.5 and 24h, achieving 55% to 41% porosity with comparatively low strength.

Axial die-compaction and isostatic pressing of powders prior to sintering increase the strength of the green body by cold welding of the particles at the contact areas. Subsequent sintering with or without applied pressure further increases the density and the strength, and the sintered compact features very fine porosity [86]. Oh et al. sintered spherical Ti powder green bodies compacted at a pressure of 70 MPa to achieve a porosity level of 5% (pressure sintering) to 37% (pressureless sintering) [87-88]. Thieme

et al. [89] reported the sintered titanium compacts with the porosity ranging from 35 to 60%, where the highest value was achieved by using agglomerated powders. Ricceri and Mateteazzi [90] used a combination of cold isostatic pressing and subsequent sintering of Ti-6Al-4V powder to produce the parts with 26% porosity; the containerless hot isostatic pressing was employed for the post-sintering treatment to eliminate the closed pores without affecting the open pores.

Electro-discharge compaction, which combines compacting and sintering of powders by applying a high density current pulse with/without external pressure, is a unique way to fabricate porous titanium and its alloy under low vacuum or even in air, due to much lower sintering temperature and time involved. Okazaki et al [91, 92] used this method to fabricate porous titanium dental implant. Kon et al [93] consolidated Ti and Ti-6Al-4V spherical powders to a porosity of 27% to 32% by this method.

Replacing titanium powders by wires opens new possibility for making porous titanium structure, which was demonstrated by sintering 30 μm diameter crimpled wire preform near 1600 °C to obtain open-cell foam with 45-50% porosity [94].

There are several limitations for the above mentioned powder sintering methods. One is that the shape and size of the pores are dictated by powder size and shape. Another is that at most 50% porosity could be achieved. The third one is that the pores are highly non-spherical in shape and cusped at the sintering necks among powders, as shown in Fig. 1, leading to easy crack initiation and low fatigue resistance due to stress concentration.

1.2 Using space holders

Space holders such as polymer spheres, magnesium granules and carbamide are mixed with titanium powders. The mixture of the titanium powders and the space holders is cold pressed, thermally treated normally at low temperature to remove the holder and then finally sintered at high temperatures (see Fig. 2).

Magnesium granules, due to the features of low boiling point (1090°C) and immiscibility in titanium, can be used as a space holder. In this process, a bulk of magnesium granules is mixed with titanium powder, followed by hot pressing the powder mixture at temperatures well below the melting point of magnesium. The magnesium granules are then removed by evaporation at temperatures up to 1400 °C at which sintering between the titanium particles takes place simultaneously [96].

Rausch et al. [97] used polymer granules as space holders, which were removed chemically at 130°C after powder compaction, to produce titanium foam with 55-80% porosity (Fig. 3). Bram et al. [98] produced highly porous titanium by using carbamide particles as space holders. A mixture of carbamide and titanium powders was prepared by adding fine titanium powder with particle size smaller than 45 μm into carbamide moistened with petroleum ethers. The mixtures were pressed at 166 MPa and heat treated first at 170°C to remove the holder, then sintered at 1400°C for 1 to 2 hours. Porosity of 60-80% and pore size of 0.1-2.5 mm were observed. Wen et al [99-101] and Laptev et al [102] used ammonium hydrogen carbonate as space holders, which can be

removed by decomposition at 200°C, to produce porous titanium with 35-80% porosity, as shown in Fig. 4.

Another alternative is to use a polymer scaffold as space holder with titanium powder slurry coated on its surface. After burning off the scaffold and binder, and subsequent sintering, a three-dimensional arrangement of hollow titanium struts is produced, as shown in Fig. 5. This method has been demonstrated by Kupp et al [103] and Li et al. [104-105]

1.3 Employing pore-forming agents

Using pore-forming agents to create pores within a titanium powder compact by releasing a gas during the foaming process is another route for making highly porous structures with large pores. Gauthier et al [106] reported their approach by molding the mixture of titanium powder, a solid polymeric binder and a foaming agent and subsequently heat treating in a three-step heat cycle including foaming, de-binding and sintering. The foaming agent starts to decompose and generates a gas when the binder melts and flows around the titanium powder. After foaming, de-binding and subsequent sintering are conducted, a titanium foam with a porosity of 66% to 79% is produced. Jee et al [107] used a two-part polyol-isocyanate foaming agent to produce a fine-celled reticulated structure with porosity greater than 90% and a pore size of 0.4mm. The selection of the proper foaming agent seems to be critical for producing high-quality titanium foams. The use of polyurethane foaming system instead of polyol-isocyanate agent left a significant amount of ash residues (3-4wt%) and contaminated the sintered titanium.

Such contaminations must be carefully controlled when a foaming agent is used. In addition, special attention should be paid to maintaining sufficient powder compact strength after compaction and pore-forming agent removal. This can be achieved by controlling the particle size of titanium and the pore-former in such a way that the size of the pore-forming particles is several times larger than the titanium particles. This will ensure sufficient number of contacts between titanium powders and therefore maintain the shape integrity of the powder compact during debinding and foaming.

1.4 Entrapped gas expansion

Entrapped gas expansion is a process in which metals or alloys are expanded in the solid state to achieve porous structures by means of building up gas pressure within small internal voids. In the process, titanium powders are packed into a can that is first evacuated and then backfilled with argon gas. The powders are then densified by hot isostatic pressing and the argon gas is entrapped in the titanium matrix in the form of isolated, micron-sized, high-pressure argon bubbles. By heating the powder compact with entrapped argon gas under vacuum at titanium's creeping or superplastic temperature leads to expansion of the entrapped gas and the formation of the titanium foam.

The entrapped gas expansion approach was first practiced by Kearns et al. [108-109] to produce Ti-6Al-4V porous structure. They found that increasing the argon backfill pressure and the heat treatment temperature for bubble expansion both increased the

porosity, as a result of significantly increased plastic deformation of of the titanium matrix at the foaming temperature. A cubic, facetted pore morphology with up to 30% porosity was obtained at 1240°C with 0.1 atm argon backfill pressure. The cubic, facetted pore morphology is the result of surface diffusion and anisotropic surface energies. They also demonstrated that the pores could be elongated by hot-working of the argon entrapped billets, which resulted in a highly anisotropic expansion upon the subsequent foaming. A variation of argon entrapment technique is the use of titanium hydride that produces hydrogen in-situ by decomposition. Ricceri and Matteazzi [110] cold-compacted a mixture of titanium powders with 5% or 10wt% TiH_2 powders and then HIP-consolidated the mixture into a billet. The internally pressurized hydrogen bubbles were formed by decomposition of TiH_2. These bubbles grew by creep deformation of the matrix at foaming temperatures (950-1150°C), resulting in a porous structure with porosity of 17-24% after 1 hour heat treatment. However, unlike the argon entrapment technique, the very high solubility and diffusivity of hydrogen in the matrix leads to rapidly reduction of the gas pressure in the H_2 bubbles and therefore reduces the driving force for foaming.

The entrapped gas expansion method has been applied by Martin et al. [111-112] for making low density core (LDC) sandwich structure by consolidating argon gas charged powder compacts followed by hot rolling and annealing to expand the gas filled pores. Fig. 6 shows schematically the implementation of the LDC process. In the process, the can was made of Ti-6Al-4V, which forms a dense outer layer of LDC, as shown in Fig. 7.

The foaming process under creeping temperature features slow kinetics and modest porosity due to the low deformation rates and the easy void coalescence. To overcome these shortcomings, attempts have been made to induce superplasticity in titanium matrix during the foaming process, aiming at faster foaming kinetics through reducing the resistance to plastic deformation, and higher final porosity by increasing the total plastic deformation. The superplasticity could be activated by thermally cycling the materials around the allotropic transformation of CP-Ti [113-115] and Ti-6Al-4V [116-118], or by chemically cycling titanium alloys through hydriding and dehydriding cycles [119]. Dunand's research group conducted a series of systematic studies [113-121] on the superplastic foaming process for titanium and Ti-6Al-4V, and examined the microstructures of the materials [115], the pore expansion kinetics [121], and the relationship between microstructure and foaming kinetics [120]. Fig. 8 shows the microstructure evolution with time during the superplastic foaming. Based on theoretical estimate, the maximum achievable porosity is 50% for creeping foaming and 65% for superplastic foaming [122-123], respectively.

2. Mechanical properties of porous titanium and its alloy

The mechanical properties of porous metals depend on the properties of the corresponding solid materials and the pore characteristics, such as porosity level, pore size, pore shape and orientation. With a wide range of pore levels and a variety of pore characteristics achievable by various fabrication processes, the mechanical properties of a porous material can be varied in a wide range. A good understanding of the relationship

between mechanical properties and pore structures is critical for properly selecting the materials and fabrication processes for intended applications.

2.1 Mechanical properties

Different processes may lead to different macro- and micro- porous structures and subsequently different mechanical properties, even though the same relative density (porosity) is obtained. Many process parameters affect the final mechanical properties of the porous titanium parts, such as the starting powder characteristics (size, size distribution, and shape), green compaction conditions (cold isostatic press, uniaxial press and compaction pressure), sintering parameters (temperature, time, ramping rate, atmosphere and pressure) and contamination controls (e.g., rapid dissolution of oxygen and nitrogen into solid titanium leads to reduction of ductility). It is desirable to discuss the mechanical properties of porous titanium materials with the underlying pore structures and compare the different fabrication techniques. However, only a limited amount of information is available on the mechanical properties of the porous titanium parts. It is difficult, based on the available information, to give the comprehensive and correct evaluations of the mechanical properties by different fabrication techniques, especially of the correlation of the mechanical properties with the pore structures. In spite of this, the results are interesting and encouraging towards the application as the porous bone-replacement implants. The main processing parameters and mechanical measurements for porous titanium and its alloy fabricated by powder sintering, using space holder and pore-forming agents and entrapped gas expansion are summarized in Table 2, Table 3 and Table 4, respectively and the following trends could be noted.

I. Lower porosity (higher relative density) leads to higher mechanical strength and higher young's elastic modulus.

II. The porosity decreases with decreasing the initial powder size.

III. Young's modulus can be tailored to match the human bone's stiffness by controlling the porosity.

In porous materials, both the strength and the Young's modulus decrease with the increase of the porosity. To meet the practical application needs, porous titanium implants with high mechanical strengths and bone-matching elastic modulus are desired. It has been demonstrated that the titanium compacts with around 30% porosity by powder sintering [87,88,93] and those with 65-80% porosity by using space holder [100] or pore-forming agent [106] have the Young's modulus close to that of human cortical bone and cancellous bone, respectively. However, the reported mechanical strength is lower than the analytical predications and no work on fatigue strength has been reported for titanium foams. A systematic investigation is needed to study the influence of various factors on the mechanical properties focusing on matching the properties with bones.

2.2 Predication of the mechanical elastic behaviors

A number of analytical methods have been developed for predicting the mechanical properties of porous materials, including Gibson-Ashby cellular mechanics method (developed for high porosity), Mori-Tanaka method (suitable for low porosity), and Brocaccini-Ondracek method (better fit for full range porosity).

Another approach for predicting the mechanical properties of porous material is employing the numerical method. In recent years, finite element analysis (FEA) has become an increasingly useful tool for the prediction of the effects of stress on the implant and its surrounding bone. FEA allows researchers to predict stress distribution within the implant itself, in the contact area of the implants with cortical bone and around the apex of the implants in trabecular bone.

2.2.1 Gibson-Ashby methods

These methods are based on the beam theory and cell wall structure, and were developed for foams and cellular materials [44]. Two major assumptions were made in these methods: (1) the walls within the porous samples are thin, or equivalently, the porosity is above approximately 70% (2) the whole porous structure can be represented by a unit cell derived from an approximate geometry. The unit cells are analyzed using simple beam theory and the global response of a repeating array of identical unit cells inferred.

The simplest structural model for cellular materials is the 2D honeycombs made up of regular hexagons (Fig. 9 (a)). The applicable expression derived from beam theory is:

$$\frac{E_p}{E} = 2.3(\frac{t}{l})^3 \qquad (1)$$

where E_p and E are the Young's modulus of the porous material and the solid material, respectively, t and l are the thickness and the length of the walls. Equation (1) can be re-written in terms of porosity as equation (2), where P is the porosity.

$$\frac{E_p}{E} = 2.3[\frac{\sqrt{3}}{2}(1-P)]^3 \qquad (2)$$

Gibson and Ashby [44] used a unit cell shown in Fig. 9 (b) to model the 3D open cell materials and obtained:

$$\frac{E_p}{E} = (1-P)^2 \qquad (3)$$

The normalized moduli calculated by various models are plotted in Figure.10 to predict the change of Young's modulus with porosity. The simple honeycomb model gives unrealistic predictions for behavior of materials with porosity <20% and the experimental data for titanium foam do not fit very well with the calculated values. It is understandable because the achieved porous structure for titanium and its alloy do not show such honeycomb structure. Therefore, 2D honeycomb model is not suitable for predicting the modulus of foams of titanium alloys. The 3D open cell model is also based on assumptions of high porosity. Experiments have shown that this model provides good predictions of modulus for autogenous titanium materials with a porosity of greater than 70% [101]. However, the Gibson-Ashby model is based on the assumption of high porosity and could not give accurate predictions for the materials with low porosity. Besides porosity level, pore characters can also have significant effects on the elastic modulus and other mechanical properties of a porous material., Thus, for accurate prediction of the effect of porosity on the modulus, the role of pore geometry (shape and orientation) on the modulus–porosity relationship ought to be taken into account.

2.2.2 *Mori-Tanaka method*

The work of Mori and Tanaka [124], originally concerned with calculating the average internal stress in the matrix of a material containing precipitates with eigenstrains, has been the basis of many micromechanics calculations [125-127]. For porous materials, the pores are treated as null-stiffness inclusions and this method has been successfully utilized for materials with up to 50% porosity. The method is derived assuming that the average strain in the pores can be approximated by that of a single pore in the matrix subjected to the average matrix strain. A recursive relationship is used along with the analytical solution for a single pore, based on the Eshelby tensor [128-129], S, which is dependent on pore shape. In the case of spherical pore, S can be calculated by:

$$S = \frac{(1+\upsilon)}{1-\upsilon} \tag{4}$$

where ν is Poisson's ratio of the matrix (when the porosity is zero).

Using this approach and neglecting any internal pressure within the pores, the expression for the effective elastic modulus of a porous material can be written as:

$$\frac{C_P}{C} = 1 - \frac{P}{(1-P)S^{-1} + P} \tag{5}$$

where C_p is the bulk or shear modulus of porous materials, C is the is bulk or shear modulus of the solid material and S^{-1} is the inverse of the Eshelby tensor. The relationship between the bulk modulus (K) and shear modulus (G) and the Young's modulus and Poisson's ratio can be given by the following relations, respectively:

$$K = \frac{E}{3-6\upsilon} \tag{6}$$

$$G = \frac{E}{2(1+\upsilon)} \qquad (7)$$

The normalized stiffness predicted by the Mori–Tanaka method for the case of spherical pores is compared with the results predicted by Gibson-Ashby methods and Brocaccini-Ondracek method in Figure 10.

2.2.3 *Brocaccini-Ondracek method*

Based on the earlier theoretical work for two-phase composite materials, Ondracek et al. [130-132] proposed a model equation for the prediction of Young's modulus of porous materials. An expression has been derived by substituting the real pore structure by a model microstructure of spheroids having the same surface to volume ratio as the real pores. Later, Boccaccini et al. [133] did a modification to extend the validity of the equation to the whole range of porosity for all possible pore structure. Two factors describing the pore structure are included in the calculation, which are the shape factor (z/x), defined by the axial ratio of the substituted spheroids and the orientation factor, defined as $\cos^2\alpha$, where α is the angle between the stress direction and the rotational axis of the substituted spheroid. The final expression for the Young's modulus of the porous materials is [133-136]:

$$\frac{E_p}{E} = (1 - P^{2/3})^{\Gamma} \qquad (8)$$

with

$$\Gamma = 1.21\left(\frac{z}{x}\right)^{1/3}\sqrt{1+\left[\left(\frac{z}{x}\right)^{-2}-1\right]\cos^2\alpha} \qquad (9)$$

For isotropic materials, $\cos^2\alpha=0.333$, as shown by Ondracek [132]. The microstructural parameters z/x and α are related to the actual features of the pore geometry and can be determined by quantitative microstructural analysis of polished sections of the material and using stereological relationships [132]. Thus, equation 8 has significant practical relevance for Young's modulus prediction in porous sintered materials. The predictive capability of the equation has been confirmed by comparison with experimental data for several porous ceramics, glasses and metals [133, 136]. For the special case of spherical pores, z/x=1 and $\cos^2\alpha=0.333$, equation 8 reduces to:

$$\frac{E_p}{E} = (1 - P^{2/3})^{1.21} \qquad (9)$$

The calculated moduli by four models are presented as a function of material porosity in Fig. 10. Principally, Brocaccini-Ondracek method is valid for the whole range of porosity for all possible porosity structure. However, there is still a noticeable discrepancy between the theoretical predications and the experimental results. This is because the pore shape is expected to change with the porosity level. Thus, it is necessary to analyze the modulus-porosity data on a point-by-point basis, thus determining at each porosity level the value of the axial ratio that provides the best fit.

2.2.4 *Finite Element Analysis (FEA) application*

FEA has been successfully used to predict the biomechanical performance of implant systems [137-140], which can include many considerations, such as the localized stress and strain field variations between the different pore structure, that the above discussed analytical models do not take into account. It was demonstrated that FEA provided the

richest information on the material mechanics because local stress field can be evaluated and the materials microstructure is more accurately represented.

2D FEA [141-142] shows that both the pore structure and bone ingrowth have significant influence on the mechanical properties of titanium foam. Slight changes of shape, size and position of pores have little influence on the Young's modulus and overall yield stress. However, randomization of pore size and spatial distribution causes the decrease of both Young's modulus and the yield strength significantly. Another important predication by 2D FEA is the impact of bone ingrowth. It was shown that bone filling remarkably improves the mechanical properties of the implant. With bone ingrowth, both Young's modulus and yield strength increase, stress concentrations decrease and plastic deformation is reduced.

It should be noted that the predications by FEA are not always consistent with the experimental measurements, especially by 2D FEA that the simplifications of 2D plane-strain approximation instead of 2D microstructures affect the predictive accuracy. The principal difficulty in simulating the mechanical behavior of implants is the modeling of human bone tissue and its response to applied mechanical force. Certain assumptions need to be made to make the modeling and solving process possible. The complexity of the mechanical characterization of bone and its interaction with implant systems has forced researchers to make major simplifications. Assumptions made in the use of FEA have to be taken into account when interpreting the results. In modeling, some assumptions greatly affect the predictive accuracy of the FEA model. These include: (1)

detailed geometry of the bone and implant to be modeled, (2) material properties, (3) boundary conditions, and (4) the interface between bone and implant [143-144]. To achieve more realistic models, advanced digital imaging techniques such as X-ray tomography [145] or magnetic resonance imaging can be used to model implant geometry in greater detail; the anisotropic and non-homogenous nature of the material needs to be considered; and boundary conditions must be refined.

4. Summary

Porous titanium and its alloys are promising biomaterials for implant applications due to their excellent biocompatibility, tailorable elastic modulus, and porous surface structures that encourage bone ingrowth and result in strong bonding between implant and surrounding tissues. The attractive features of porous titanium and its alloys have led to strong interest in such materials and significant research efforts in developing fabrication technologies and the characterization of their properties.

Generally porous titanium alloys can only be fabricated by powder metallurgy because of the high melting temperature and the high reactivity of titanium. Partial sintering of titanium powders or wire can lead to 20-50% porosity with the limitation of highly non-spherical pores at the high porosity and therefore the low mechanical strength. The approach using space-holders or pore-forming agents can produce titanium foam with the adjustable pore structure and high porosity up to 90%, but the contaminations caused by the space-holder or agents must be carefully controlled. Entrapped gas expansion under creeping temperature exhibits slow kinetics and modest porosity. The foaming process

can be accelerated by superplastic thermal cycling that can also lead to a higher final porosity level.

Porous titanium materials with Young's modulus close to human's cortical and cancellous bones and suitable mechanical strength can be fabricated by the adjustment of porosity and processing parameters. However, the overall mechanical performance of the porous titanium is not yet satisfactorily evaluated. Further improvements in the mechanical properties are needed for the materials to be used for load-bearing implant.

Among the different analytical methods, Gibson-Ashby method is simple and works well for high porosity titanium foams. Mori-Tanaka method and Brocaccini-Ondracek method have the advantages of being able to account for the pore geometry, which can give better predications for elastic modulus. Numerical analysis based on finite elements analysis can predict the stress/strain distribution within the implant itself and the surface area of the implant contacted with the surrounding bones. It has shown that once the bone ingrowth is achieved in the porous implant, the localized stress concentrations are dramatically decreased and consequently longer lifetime and decreased failure rate of an implant.

References:

1. J.C. Van Loon, Titanium, in *Encyclopedia Americana,* Vol 26, Grolier, 1984, p 785
2. G.C. Leventhal, Titanium--A Metal for Surgery, *J. Bone Joint Surg.,* Vol 33, 1951, p 473
3. G.H. Hille, Titanium for Surgical Implants, *J. Met.,* Vol 1 (No. 2), 1966, p 373-383
4. J.A. McMaster, "Titanium for Prosthetic Devices," Paper presented at the Dental-Medical Committee Meeting, Cleveland, OH, American Institute of Mining, Metallurgical and Petroleum Engineers, Oct 1970
5. D.F. Williams, Titanium and Titanium Alloys, in *Biocompatibility of Clinical Implant Materials,* Vol 1, D.F. Williams, Ed., CRC Press, 1981, p 9-44
6. J. Black and G.W. Hastings, Handbook of Biomaterials Properties, London, UK: Chapman and Hall, 1998.
7. D.M. Brunette, P. Tengvall, M. Textor, P. Thomsen , Titanium in Medicine, Springer, Berlin Heidelberg New York, 2001
8. Galante JO, Jacobs J. Clinical performance of ingrowth surfaces. *Clin Orthop* 1992;276:41– 49.
9. S.F. Hulbert, S.D. Cook. The case of a composite hip prosthesis. In: Vincenzini P, editor. Ceramics in substitutive and reconstructive surgery. Amsterdam: Elsevier; 1991. p 545–565
10. R.M. Pilliar, J.M. Lee and C. Maniatopoulos, Observation on the effect of movement on bone ingrwoth into porous surfaced implants, *Clin. Orthop.*, 208(1986)p.108-113.
11. S. Szmukler–Moncler, H. Salama, Y. Reingewirtz, J. H. Dubruille, Timing of loading and effect of micromotion on bone-dental implant interface: Review of experimental literature, *J Biomed Mater Res.,* 43(1998) 192.
12. A. Wennerberg, T. Albrektsson, C. Johansson, B. Andersson. Experimental study of turned and grit-blasted screw-shaped implants with special emphasis on effects of blasting material and surface topography. *Biomaterials*, 17(1996)15.
13. A. Wennerberg, T. Albrektsson, J. Lausmaa, Torque and histomorphometric evaluation of c.p. titanium screws blasted with 25- and 75-mm-sized particles of Al_2O_3. *J Biomed Mater Res,* 30(1996)251.
14. F. Guillemot, M. C. Porté, C. Labrugère and Ch. Baquey, Ti^{4+} to Ti^{3+} Conversion of TiO_2 Uppermost Layer by Low-Temperature Vacuum Annealing: Interest for Titanium Biomedical Applications, *Journal of Colloid and Interface Science,* 255(2002)75.
15. Shunsuke Fujibayashi, Masashi Neo, Hyun-Min Kim, Tadashi Kokubo and TakashiNakamura, Osteoinduction of porous bioactive titanium metal, *Biomaterials,* 25(2004)443.
16. Limin Sun, Christopher C. Berndt, Karlis A. Gross, Ahmet Kucuk, Material fundamentals and clinical performance of plasma-sprayed hydroxyapatite coatings: A review, *J. Biomed. Mater. Res.* 58(2001)570.

17. Kenzo Asaoka, Norihiko Kuwayama, Osamu Okuno, Ishi Miura, Mechanical properties and biomechanical compatibility of porous titanium for dental implants, *J. Biomed. Mater. Res.* vol. 19(1985)699.
18. S. Yue, R. M. Pilliar, G. C. Weatherly, The fatigue strength of porous-coated Ti-6% Al-4% V implant alloy *J. Biomed. Mater. Res.* 18(1984)1043.
19. W. H. Lee and D.A. Puleo, Mechanism of consolidation of a porous-surfaced Ti-6Al-4V implant formed by electrodischarg compaction, *J. mater. Sci. Lett.* 18(1999)817.
20. R.M. Pilliar, Powder metal-made orthopaedic implants with porous surfaces for fixation by tissue ingrowth, *Clin. Orthop.*, 176(1983)42.
21. H. U. Cameron, R.M. Pilliar and I. macnab, The effect of movement on the bonding of porous metal to bone, *J. Biomed. Mater. Res.* 7(1973)301.
22. R.M. Pilliar, H.U. Cameron, R.P. Welsh and A.G. Binnington, Radiographic and Morphologic Studies of Load-bearing Porous Surface Structure implants, *Clin. Orthop.*, 156(1981)249.
23. J.J. Klawitter, and S.F. Hulbert, Application of porous ceramics for the attachment of load bearing internal orthopedic application, *J. Biomed. Mater. Res. Symposia,* 2(1971)161.
24. J.D. Bobyn, R.M. Pilliar, H.U. Cameron and G.C. Weatherly, The optimum pore size for fixation of porous surfaced metal implants by the ingrowth of bone, *Clin. Orthop.*, 149(1980)291..
25. D.S. Hungerford, R.V. Kenna, Preliminary experience with a total knee prosthesis with porous coating used without cement, *Clin. Orthop.*, 176(1983)95.
26. C.A. Engh, Hip Arthroplast with a Moore Prosthesis with porous coating, *Clin. Orthop.*, 176(1983)52.
27. M. Long and H.J. Rack, Titanium Alloys in Total Joint Replacement—A Materials Science Perspective, *Biomaterials*, 19 (1998)1621.
28. D.R. Sumner and J.O. Galante, *Clinical Orthopedics Related Research*, 274 (1992)202.
29. A.R. Dujovne, J.D. Bobyn, J.J. Krygier, J.E. Miller and C.E. Brooks, Mechanical compatibility of noncemented hip prostheses with the human femur. *J Arthroplasty*; 8(1993)7.
30. C.A. Engh and J.D. Bobyn, The infuence of stem size and extent of porous coating on femoral bone resorption after primary cementless hip arthroplasty. *Clin Orthop Relat Res*; 231(1988)7.
31. E.J. Cheal, M. Spector, W.C. Hayes. Role of loads and prosthesis material properties on the mechanics of the proximal femur after total hip arthroplasty. *J Orthop Res,* 10(1992)405.
32. R. Huiskes, H. Weinans, B. van Rietbergen. The relationship between stress shielding and bone resorption around total hip stems and the elects of flexible materials. *Clin Orthop Relat Res*; 274(1992)124.
33. D.R. Sumner, J.O. Galante. Determinants of stress shielding: design versus materials versus interface. *Clin Orthop Relat Res* , 274(1992)202.
34. K. Shigery, T. Oku and S. Takagi. Hydraulic property of hydroxyapatite thermal decomposition product and its application as a biomaterial. *J. Ceram Soc Japan Inter Ed.*, 97(1989)96.

35. W. Bonfield, , M.D. Grynpas, A.E. Tully, J. Bowman, and J. Abram, Hydroxyapatite reinforced polyethylene - a mechanically compatible implant for bone replacement. *Biomaterials*, 2 (1981)185.
36. I. Ono, T. Tateshita, and T. Nakajima, Evaluation of a high-density polyethylene fixing system for hydroxyapatite ceramic implants. *Biomaterials*, 21(2000)143.
37. M. Marcolongo, P. Ducheyne, J. Garino and E. Schepers Bioactive glass fiber/polymeric composites bond to bone tissue *J Biomed Mater Res*, 39(1998)161.
38. P Christel, A Meunier, S Leclercq, P Bouquet, B Buttazzoni Development of a carbon-carbon hip prosthesis, *J Biomed Mater Res.* 1987 Aug;21(A2 Suppl):191-218.
39. J.A. de Oliveira Simoes, A.T. Marques, Determination of stiffness properties of braided composites for the design of a hip prosthesis, *Composites: Part A* 32 (2001)655.
40. R. Davidson, S. Brabon, R.J. Lee, K. Nelson, P. Unwin and P. Roughley. The development of CFRP based hip stems. Proc. of the 7th European Conf. on Composite Mater., London, 1996, p.513-517.
41. F.K. Chang, J.L. Perez, JA Davidson, Stiffness and strength tailoring of a hip prosthesis made of advanced composite materials. *J Biomed Mater Res.* 24(1990)873.
42. T. Ahmed et al., *Titanium 95: Science and Technology*, ed. P.A. Blenkinsop, W.J. Evans, and H.M. Flower (London: IoM, 1995), pp. 1760–1767.
43. J.I. Qazi, B. Marquardt, and H.J. Rack, High-Strength Metastable Beta-Titanium Alloys for Biomedical Applications, *JOM*, Nov. 2004, p.49-51.
44. L.J. Gibson and M.F. Ashby, *Cellular Solids:Structure and Properties,* 2nd ed. CambridgeUniversity Press, Cambridge, 1997.
45. G.J. Davies, S. Zhen, Metallic Foams: Their Production, Properties and Applications. *J Mater Sci,* 18(1983)1899.
46. J Banhart, Manufacture, characterization and application of cellular metals and metal foams, *Progress in Materials Science*, 46(2001)559.
47. I. Jin, L.D. Kenny, H. Sang, US Patent 4,973,358, 1990.
48. W. Ruch, B. Kirkevag European Patent Application EP 0,483,184, B1, 1991.
49. I. Jin, L.D. Kenny, H. Sang US Patent 5,112,697, 1992.
50. M. Thomas, L.D. Kenny, H. Sang Int. Patent Application WO 94/17218, 1994.
51. H. Sang, M. Thomas, L.D. Kenny, Int. Patent Application WO 92/03582, 1992.
52. P. Åsholt, Metallschäume. In: Banhart J, editor. Proc. Symp. Metallschaume, Bremen, Germany, 6–7 March. Bremen: MIT Press–Verlag, 1997. p. 27
53. J. Wood, Metal foams. In: Banhart J, Eifert H, editors. Proc. Fraunhofer USA Symposium on Metal Foams, Stanton, USA, 7–8 October. Bremen: MIT Press–Verlag, 1998. p. 31.
54. P. Asholt, Metal foams and porous metal structures. In: J. Banhart, M.F. Ashby, N.A. Fleck, editors. Int. Conf., Bremen, Germany, 14–16 June. Bremen: MIT Press–Verlag, 1999. p. 133.
55. J.C. Elliot, US Patent 2,983,597, 1961.
56. W.S Fiedler, US Patent 3,214,265, 1965.
57. P.W. Hardy, G.W. Peisker, US Patent 3,300,296, 1967.

58. C.B. Berry, US Patent 3,669,654, 1972.
59. J. Bjorksten, E.J. Rock, US Patent 3,707,367, 1972.
60. F. von Zeppelin, M. Hirscher, H. Stanzick and J. Banhart, Desorption of hydrogen from blowing agents used for foaming metals, *Composite Science and Technology*. 63(2003) 2293-2300.
61. V.I. Shapovalov, US Patent 5,181,549, 1993.
62. V.I. Shapovalov, Porous and cellular materials for structural applications. In: D.S. Schwartz, D.S. Shih, A.G. Evans, H.N.G. Wadley, editors. *MRS Symp. Proc.,* vol. 521, 1998. p. 281.
63. A. Pattnaik, S.C. Sanday, C.L. Vold, H.I. Aaronson. Advances in porous materials. In: S. Komarneni, et al., editors. MRS Symp. Proc., vol. 371, 1995. p. 371.
64. J.M. Wolla, V. Provenzano, Advances in porous materials. In: S. Komarneni, et al., editors. MRS Symp. Proc., vol. 371, 1995. p. 377.
65. V. Provenzano, J. Wolla, P. Matic, A. Geltmacher, A. Kee. Advances in porous materials. In: S. Komarneni, et al., editors. MRS Symp. Proc., vol. 371, 1995. p. 383.
66. A.E. Simone, L.J. Gibson, The tensile strength of porous copper made by the GASAR process, *Acta Met*, 44(1996)1437.
67. A.E. Simone, L.J. Gibson, Compressive behaviour of porous copper made by the GASAR process, *J Mat Sci*, 32(1997)451.
68. C.J. Paradies, A. Tobin, J. Wolla. Porous and cellular materials for structural applications. In: D.S. Schwartz, D.S. Shih, A.G. Evans, H.N.G. Wadley, editors. MRS Symp. Proc., vol. 521, 1998. p.297.
69. R.J. Bonenberger, A.J. Kee, R.K. Everett, P. Matic. Porous and cellular materials for structural applications. In: D.S. Schwartz, D.S. Shih, A.G. Evans, H.N.G. Wadley, editors. MRS Symp. Proc., vol. 521, 1998. p. 303.
70. C. Park, S.V. Nutt. Porous and cellular materials for structural applications. In: D.S. Schwartz, D.S. Shih, A.G. Evans, H.N.G. Wadley, editors. MRS Symp. Proc., vol. 521, 1998. p. 315.
71. J. Banhart, J. Baumeister, M. Weber, Euro. Conf. Advanced PM Materials (PM '95), Birmingham, UK, 23–25 October 1995. p. 201.
72. I. Duarte, P. Weigand, J. Banhart,Metal foams and porous metal structures. In: J. Banhart, M.F. Ashby, N.A. Fleck, editors. Int. Conf., Bremen, Germany, 14–16 June. Bremen: MIT Press–Verlag,1999. p. 97.
73. J. Banhart, J. Baumeister, M. Weber, Metal powder technologies and applications. In: ASM handbook, vol. 7. Materials Park, USA: ASM International, 1998. p. 1043.
74. I. Duarte, J. Banhart, A study of aluminium foam formation-kinetics and microstructure, *Acta Mater,* 48(2000)2349.
75. J.R. Kreigh, J.K. Gibson. US Patent 3,055,763, 1962.
76. H.A. Kuchek, US Patent 3,236,706, 1966.
77. J. Banhart, *Aluminum 75(*1999)1094.
78. F. Chen, D.P. He. Metal foams and porous metal structures. In: J. Banhart, M.F. Ashby, N.A. Fleck, editors. Int. Conf., Bremen, Germany, 14–16 June. Bremen: MIT Press–Verlag, 1999. p. 163.

79. W. Thiele, Aluminium used as an impact energy absorbing material, *Metals and Materials*, 6(1972)349.
80. W.J. Drury, S.A. Rickles, T.H. Sanders, J.K. Cochran In: E.W. Lee, E.H. Chin, N.J. Kim, editors. Proc. Conf. Light alloys for Aerospace Applications, Las Vegas, USA, 28 February–2 March, 1989. p.311.
81. S.P. Rawal, B.R. Lanning, M.S. Misra . Proc. Conf. ICCM/9, Zaragoza, Spain, 12–16 July1993, vol.1:203.
82. M. Hartmann, K. Reindel, R.F. Singer. Porous and cellular materials for structural applications. In: D.S. Schwartz, D.S. Shih, A.G. Evans, H.N.G. Wadley, editors. MRS Symp. Proc., vol. 521, 1998. p. 211.
83. Y. Yosida, C. Hayashi, Conf. Casting Science and Technology, September 1990. p. 103.
84. Y. Yamada, K. Shimojima, Y. Sakaguchi, M. Mabuchi, M. Nakamura, T. Asahina, Mukai T, Kanahashi H, Higashi K. *Advanced Engineering Materials* 2(2000)184.
85. R. Cirincione, R. Anderson, J. Zhou, D. Mumm, W.O. Soboyejo, in processing and properties of lightweight cellular Metals and Structures, Eds: A. Ghosh, T. Sanders and D. Claar, *TMS*, Warrendale, 2002, p189.
86. M. Eisenmann, Metal powder technologies and applications. In: *ASM Handbook, vol. 7*. Materials Pack, USA: ASM International, 1998. p. 1031.
87. I.H. Oh, N. Nomura, and S. Hanada,. Microstructure s and Mechanical Properties of Porous titanium Compacts Prepared by Powder Sintering, *Mater. Trans.* 43(2002)443.
88. I.H. Oh, N. Nomura, N. Masahashi and S. Hanada, Mechanical properties of porous titanium compacts prepared by powder sintering, vol. *Scripta Mater.* 49(2003)1197.
89. M. Thieme, K.P. Wieters, F. Bergner, D. Scharnweber, H. Worch, J. Ndop, T.J. Kim, W. Grill, Titanium powder sintering for preparation of a porous functionally graded material destined for orthopaedic implants *J. Mater. Sci.-Mater. Med.* 12(2001)225.
90. R. Ricceri and P. Matteazzi, Porous nano-crystalline Ti-alloy implants, *Intern. J. Powder Metall.* 37(2001)61.
91. K. Okazaki, W.H.Lee, D.K. kim and R.A. Kopczyk, Physical Characteristics of Ti-6Al-4V Implants Fabricated by Electrodischarge Compaction, *J. Biomed. Mater. Res.* 25(1991)1471.
92. J. Qiu, J.T. Dominici, M.I. Lifland and K. Okazaki, Composite titanium dental implant fabricated by electro-discharge compaction, *Biomaterial*, 18(1997)153.
93. M. Kon, L.M. Hirakata and K. Asaoka, Porous Ti-6Al-4V alloy fabricated by spark plasma sintering for biomimetic surface modification, *J. Biomed. Mater. Res.* 68(2004)88.
94. G.A.W. Murray and J. C. Semple, *J. Bone Joint Surg.-Br.* 63(1981)138.
95. N. Taylor, D. C. Dunand and A. Mortensen, Initial stage hot pressing of monosized Ti and 90% Ti-10% TiC powders, *Acta metal. Mater.* 41(1993)955.
96. K.R. Wheeler, M.T. Karagianes, K.R. Sump *Conf. Titanium Alloys in Surgical Implants*. Philadelphia, USA: American Society for Testing and Materials, 1983. p. 241.

97. G. Rausch and J. Banhart, Handbook of Cellular Metals, Eds by H.P. Degischer and B. Kriszt, Wiley, 2002.
98. M. Bram, C. Stiller, H. P. Buchkremer, D. Stöver, H. Baur, High-Porosity Titanium, Stainless Steel, and Superalloy Parts, *Adv. Eng. Mater.* 2(2000)196.
99. C. E. Wen, M. Mabuchi, Y. Yamada, K. Shimojima, Y. Chino and T. Asahina, Processing of biocompatible porous Ti and Mg, *Scripta Materialia,* 45(2001)1147.
100. C.E. Wen, Y. Yamada, K. Shimojima, Y. Chino, H. Hosokawa, and M. Mabuchi, Novel titanium foam for bone tissue engineering, *J. Mater. Res.* 17(2002)2633
101. C.E. Wen, Y. Yamada, K. Shimojima, Y. Chino, T. Asahina and M. Mabuchi, Processing and Mechanical Properties of Autogenous Titanium Implant materials, *J. Mater. Sci.: Mater. Med.* 13(2002)397.
102. A. Laptev; M. Bram; H. P. Buchkremer; D. Stöver, Study of production route for titanium parts combining very high porosity and complex shape, *Powder Metallurgy*, 47(2004)85.
103. D. Kupp, D. Claar, K. Flemming, U. Waag, H. Goehler, in Processing and Properties of Lightweight Cellular Metals and Structures, Eds: A. Ghosh, T. Sanders and D. Claar, *TMS*, Warrendale, 2002, p.61
104. J.P. Li, S.H. Li, Klaas de Groot and P. Layrolle, Preparation and Characterization of Porous Titanium, *Key Engr. Mater.* 218-220(2002)51.
105. J.P. Li, S.H. Li, Klaas de Groot and P. Layrolle, Improvement of Porous Titanium with Thicker Struts *Key Engr. Mater.* 240-242(2003)547.
106. M. Gauthier, R. Menini, M. Bureau, S.K.V. So, M.-J. Dion, L.P. Lefebvre, Properties of Novel Titanium Foams Intended for Biomedical Applications, *Proceedings from the Materials & Processes for Medical Devices Conference, Sep. 2003, Anaheim, California* , p. 382.
107. C.S.Y Jee; N. Özgüven; Z.X. Guo; J.R.G. Evans, Preparation of High Porosity Metal Foams, *Metall. & Mater. Trans.* , 31(2000)1345.
108. M.W. Kearns, P.A. Blenkinshop, A.C. Barber, T.W. Farthing, Manufacture of a novel porous metal, *Metals Mater.* 3(1987)85.
109. M.W. Kearns, P.A. Blenkinsop, A.C. Barber, T.W. Farthing, Manufacture of a novel porous metal, *Int J Powder Met* 24(1988)59.
110. R. Ricceri, P.Matteazzi, *Intern. J. Powder Metall.* 39(2003)53.
111. R.L. Martin, R.J. Lederich. Porous core/be Ti-6.4 development for aerospace structures, *Advances in Powder Metallurgy*, v 6, *Aerospace, Refractory and Advanced Materials*, 1991, p. 361.
112. D.S. Schwartz, D.S. Shih, R.J. Lederich, R.L. Martin, D.A. Deuser. Porous and cellular materials for structural applications. In: D.S. Schwartz, D.S. Shih, A.G. Evans, H.N.G. Wadley, editors. *MRS Symp. Proc.,* vol. 521, 1998. p. 225.
113. D. C. Dunand and C. M. Bedell, Transformation-mismatch superplasticity in reinforced and unreinforced titanium, *Acta Meter,* 44(1966)1063.
114. N.G. Davis, J. Teisen, C. Schuh, D.C. Dunand, Solid-state foaming of titanium by superplastic expansion of argon-filled pores, *J. Mater. Res.* 16(2001)1508.
115. N.G.D. Murray, D.C. Dunand, Microstructure evolution during solid-state foaming of titanium, *Comp. Sci. & Tech.* 63(2003)2311.

116. Megan Frary, Christopher Schuh, and David C. Dunand, Kinetics of Biaxial Dome Formation by Transformation Superplasticity of Titanium Alloys and Composites, *Metall. Mater. Trans. A* 33(2002)1669.
117. C. Schuh, D.C. Dunand Tensile fracture during transformation superplasticity of Ti-6Al-4V, *J. Mater. Res.* 16(2001)865.
118. C. Schuh and D. C. Dunand, Load transfer during transformation superplasticity of Ti–6Al–4V/TiB whisker-reinforced composites, *Scripta Mater.* 45(2001)631.
119. N. G. D. Murray, C. A. Schuh and D. C. Dunand, Solid-state foaming of titanium by hydrogen-induced internal-stress superplasticity, , *Scripta Mater.* 49(2003)879.
120. N. G. D. Murray and D. C. Dunand, Effect of thermal history on the superplastic expansion of argon-filled pores in titanium: Part I kinetics and microstructure, *Acta Meter,*52(2004)2269.
121. N. G. D. Murray and D. C. Dunand, Effect of thermal history on the superplastic expansion of argon-filled pores in titanium: Part II modeling of kinetics *Acta Meter,*52(2004)2279.
122. Douglas T. Queheillalt; Bill W. Choi; Daniel S. Schwartz; Haydn N.G. Wadley Creep Expansion of Porous Ti-6Al-4V Sandwich Structures, *Metall. Mater. Trans. A* 31(2000)261.
123. D. M. Elzey and H. N. G. Wadley The Limits Of Solid State Foaming, *Acta mater.* 49 (2001) 849.
124. T. Mori, K. Tanaka, Average stress in matrix and average elastic energy of materials with misfitting inclusions. *Acta Metall* 21(1973)571
125. D. Weng, Some elastic properties of reinforced solids, with special reference to isotropic ones containing spherical inclusions. *Int J Eng Sci*, 22(1984)845
126. Y. Benveniste, A new approach to the application of Mori–Tanaka's theory in composite materials. *Mech Mater* 6(1987)147.
127. J. Aboudi, Mechanics of composite materials: a unified micromechanical approach. Amsterdam: Elsevier; 1991
128. J.D. Eshelby, The determination of the elastic field of an ellipsoidal inclusion, and related problems. *Proc Royal Soc London*, A(241), 1957, p376 –396.
129. T. Mura, Micromechanics of defects in solids. Boston, MA: Kluwer Academic; 1987.
130. G. Ondracek, Microstructure-Thermomechanical-Property Correlations of Two-phase and Porous Materials, *Mater. Chem.& Phys.* 15(1986)281.
131. P. Mazilu and G. Ondracek, in Thermal Effects in Fracture of Multiphase Materials, *Proc. Euromech Colloquium 255*, Eds, K. Herrman and Z. Olesiak, Springer Verlag, Heidelberg, Tokyo, New York, 1989, pp.214-230.
132. G. Ondracek, *Rev. Powder Metall. Phys. Ceram.* 3(1987) 205.
133. A. R. Boccaccini, g. Ondracek, p. Mazilu and d. Windelberg, *J. Mech. Behav. Mater.* 4 (1993) 119.
134. M. Arnold, a. R. Boccaccini and g. Ondracek, Prediction of the Poisson's ratio of porous materials, *J. Mater. Sci.* 31 (1996) 1643.
135. D.N. Boccaccini and A.R. Boccaccini Effect of pore shape on the ultrasonic velocity-porosity correlation in sintered materials. *J. Mater. Sci. Let.* 16(1997) 623.

136. D.N. Boccaccini and A.R. Boccaccini, Dependence of ultrasonic velocity on porosity and pore shape in sintered materials, *J. Nondestructive Evaluation* 16(1997)187.
137. H.D. Gans, P.R. Woodmansee. Improved method of modeling porous materials using finite elements. Comput Struct Mech Mater Biomater 44(1992)1055.
138. S. Moorthy, S. Ghosh. Model for analysis of arbitrary composite and porous microstructures with voronoi cell finite elements. *Int J Numer Methods Eng Metal Powder Rep* 39(1996)2363.
139. S.J. Hollister, J.M. Brennan, N. Kikuchi. A homogenization sampling procedure for calculating trabecular bone effective stiffness and tissue-level stress. *J Biomech* 27(1994)433.
140. X.E. Guo, T.A. McMahon, T.M. Keaveny, W.C. Hayes, L.J. Gibson. Finite element modelling of damage accumulation in trabecular bone under cyclic loading. *J Biomech* 27(1994)45.
141. H. Li, S.M.Oppenheimer, S.I. Stupp, D.C. Dunand and L.C. Brinson, Effects of pore morphology and bone ingrowth on mechanical properties of microporous titanium as orthopaedic implant material, *Mater. Trans.* 45(2004)1124.
142. S. Thelen, F. Barthelat and L.C. Brinson, Mechanics considerations for microporous titanium as an orthopedic implant material, *J Biomed Mater Res* 69A(2004)601.
143. T.W. Korioth, A. Versluis, Modeling the mechanical behavior of the jaws and their related structures by finite element (FE) analysis. *Crit Rev Oral Biol Med* 8(1997)90.
144. Van Oosterwyck H, Duyck J, Vander Sloten J, Van der Perre G, De Cooman M, Lievens S, et al. The influence of bone mechanical properties and implant fixation upon bone loading around oral implants. *Clin Oral Implants Res.* 9(1998)407.
145. E. Maire, A. Fazekasb, L. Salvob, R. Dendievelb, S. Youssefa, P. Cloetensc, J.M. Letangd, X-ray tomography applied to the characterization of cellular materials. Related finite element modeling problems, *Compo. Sci. & Tech.* 63(2003)2431.

Figure Captions

Fig. 1 Cross-section of porous titanium compact produced by partial sintering of CP-Ti powder to show the sharply cusped pore feature (courtesy, Taylor et al. [95]).

Fig. 2. Space holder technique for making porous metallic structures from metal powders (adapted from Ref. [98]).

Fig. 3 Titanium foam made by powder metallurgy using polymer (left) or magnesium granules (right) as space holder (courtesy, Banhart et al. [46]).

Fig. 4 Structure of porous titanium with various volume percent space holder (a) 0%, (b) 30%, (c) 50%, (d) 70% (courtesy, Laptev et al. [102]).

Fig. 5 Ti-6Al-4V foam prepared by sintering of powder deposited on a fugitive scaffold (courtesy, Li et al. [104]).

Fig. 6 Schematic drawing to show the LDC process. [110]

Fig. 7 Ti-6Al-4V sandwich structure with a porous core (courtesy, Schwartz et al. [112]).

Fig. 8 Microstructure evolution during superplastic entrapped gas expansion of CP-Ti (a) 0 h, (b) 8 h, (c) 26 h, (d) 83 h (courtesy, Murray et al. [115]).

Fig. 9 The unit cells used by Gibson and Ashby to model the foam and cellular materials [44] (a) 2D hexagonal honeycomb cell, (b) 3D cubic open cell.

Fig. 10. Theoretical predictions for the Young's modulus using the various models.

Table Captions

Table 1: Comparison of mechanical properties of typical metallic and ceramic biomaterials with human bones. [6]

Table 2.: Summary of processing and mechanical results for porous titanium and its alloy compacts by powder sintering.

Table 3: Summary of processing and mechanical results for porous titanium and its alloy compacts by using space holder or pore-forming agents.

Table 4: Summary of processing and mechanical results for porous titanium and its alloy compacts by entrapped gas expansion.

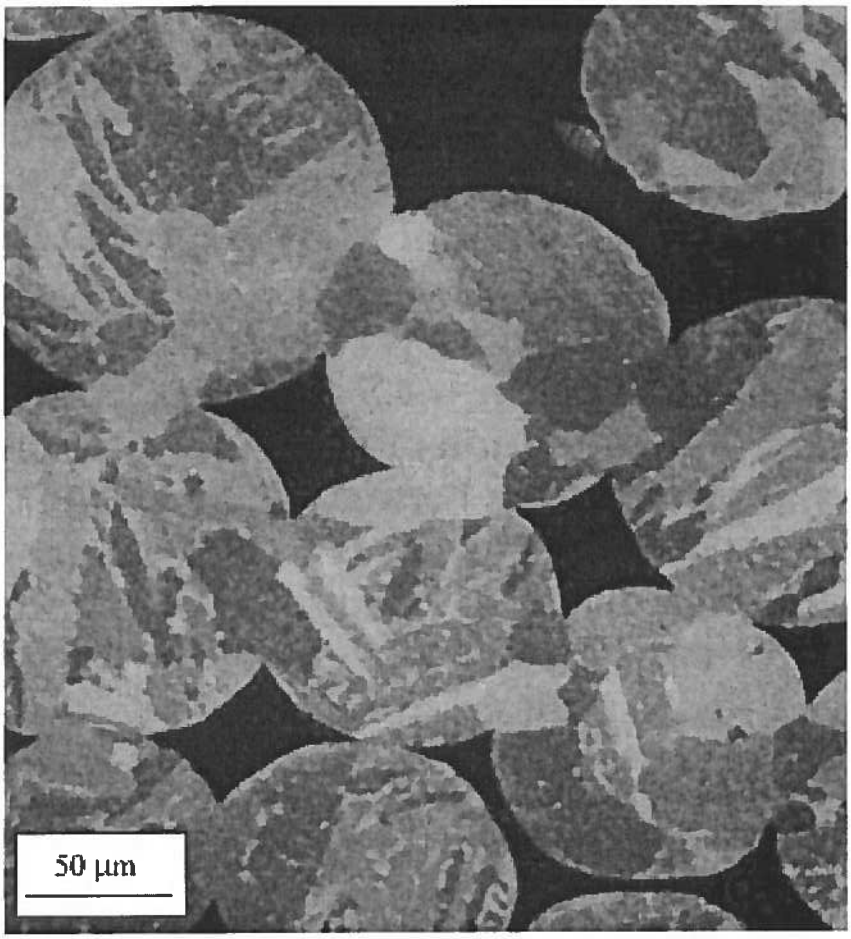

Fig. 1 Cross-section of porous titanium compact produced by partial sintering of CP-Ti powder to show the sharply cusped pore feature (courtesy, Taylor et al. [95]).

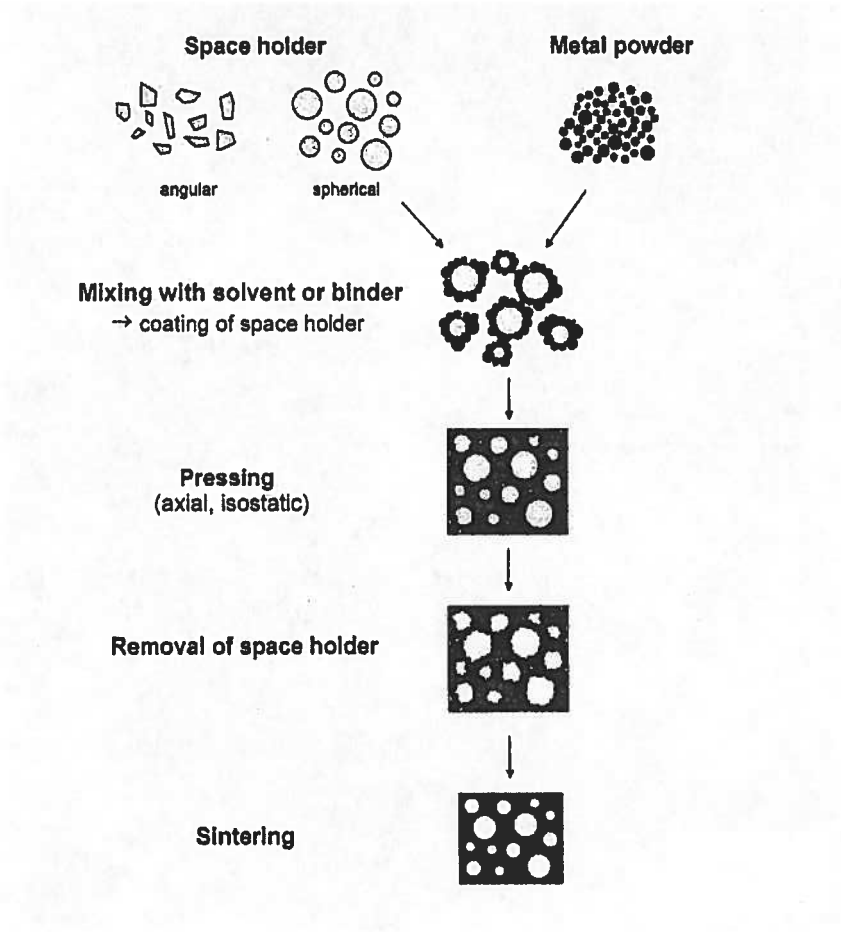

Fig. 2 Space holder technique for making porous metallic structures from metal powders (adapted from Ref. [98]).

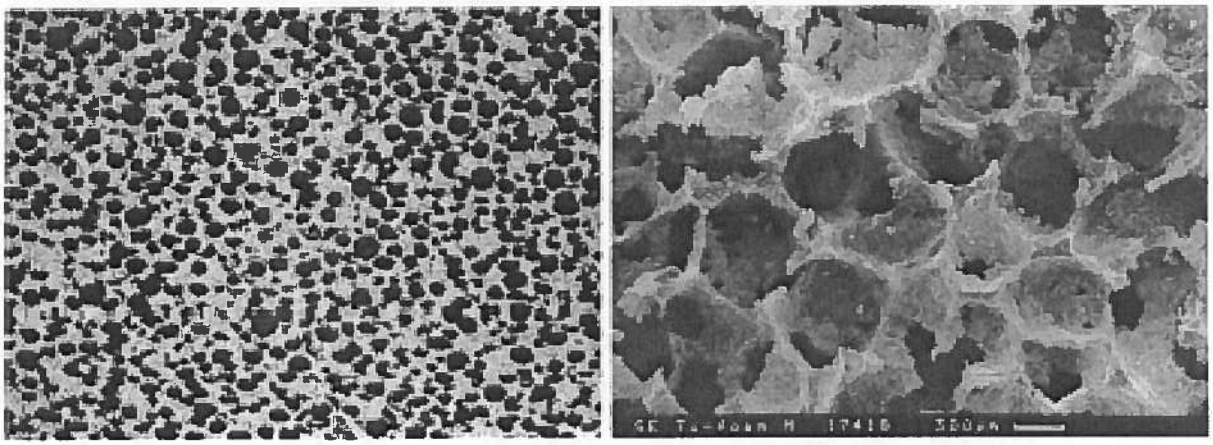

Fig. 3 Titanium foam made by powder metallurgy using polymer (left) or magnesium granules (right) as space holder (courtesy, Banhart et al. [46]).

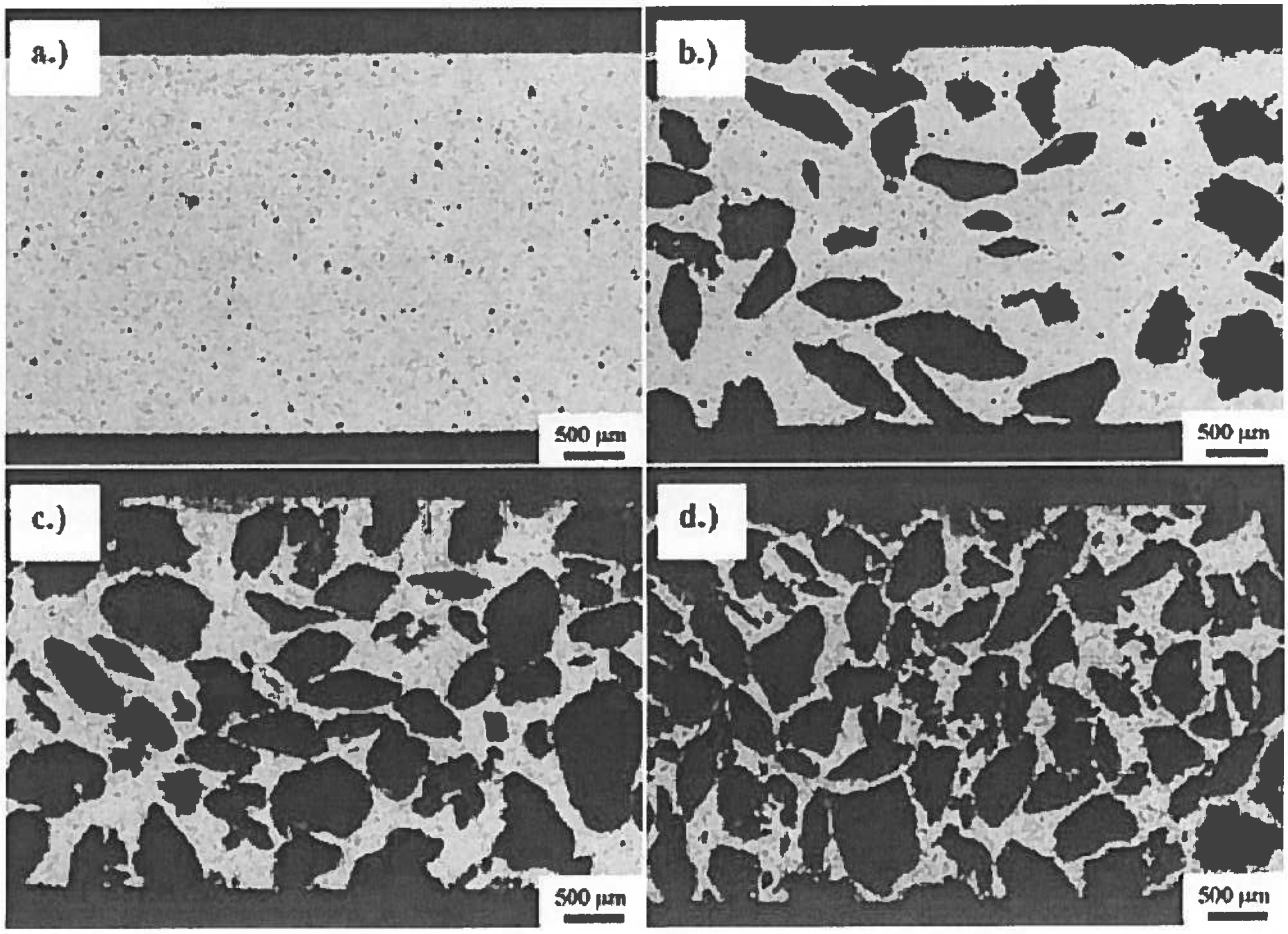

Fig. 4 Structure of porous titanium with various volume percent space holder (a) 0%, (b) 30%, (c) 50%, (d) 70% (courtesy, Laptev et al. [102]).

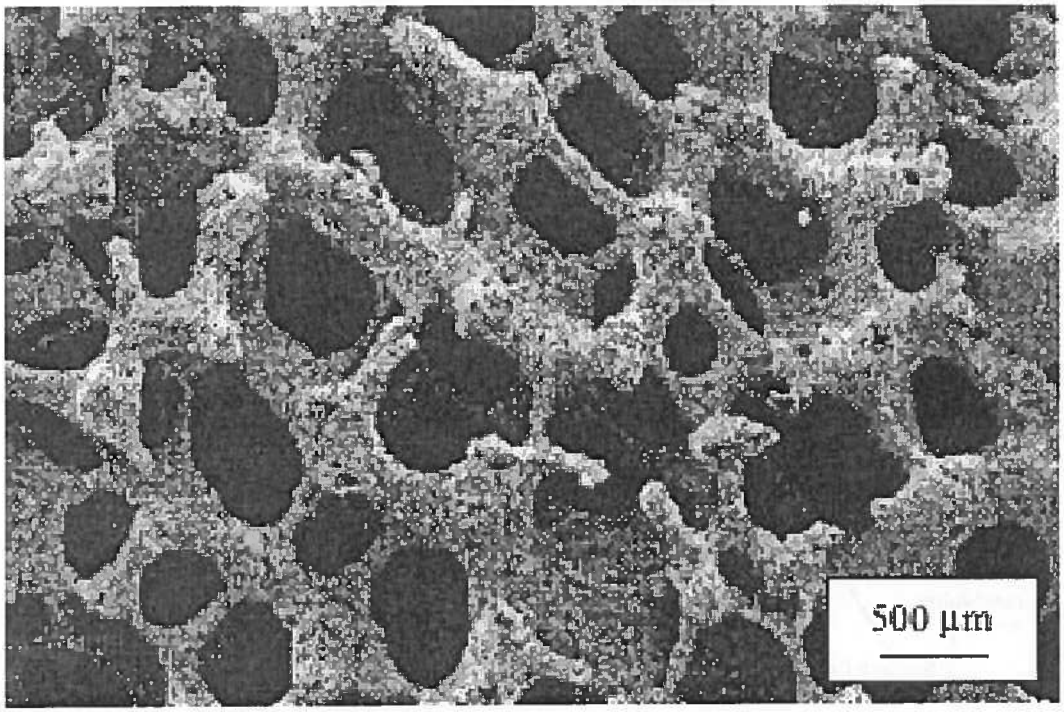

Fig. 5 Ti-6Al-4V foam prepared by sintering of powder deposited on a fugitive scaffold (courtesy, Li et al. [104]).

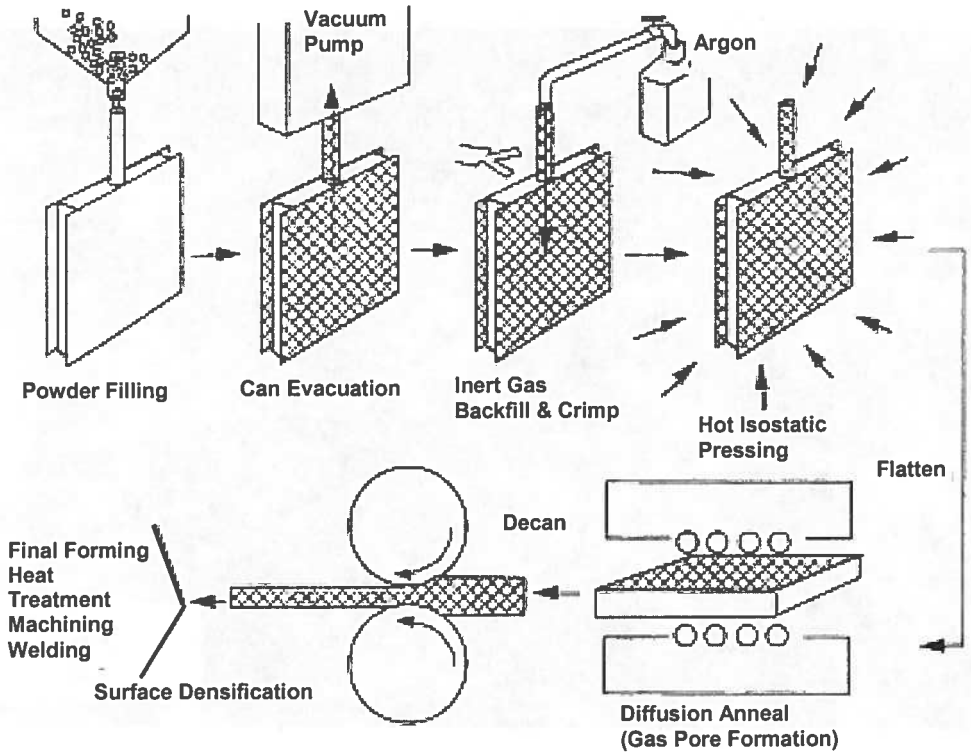

Fig. 6 Schematic drawing to show the LDC process. [110]

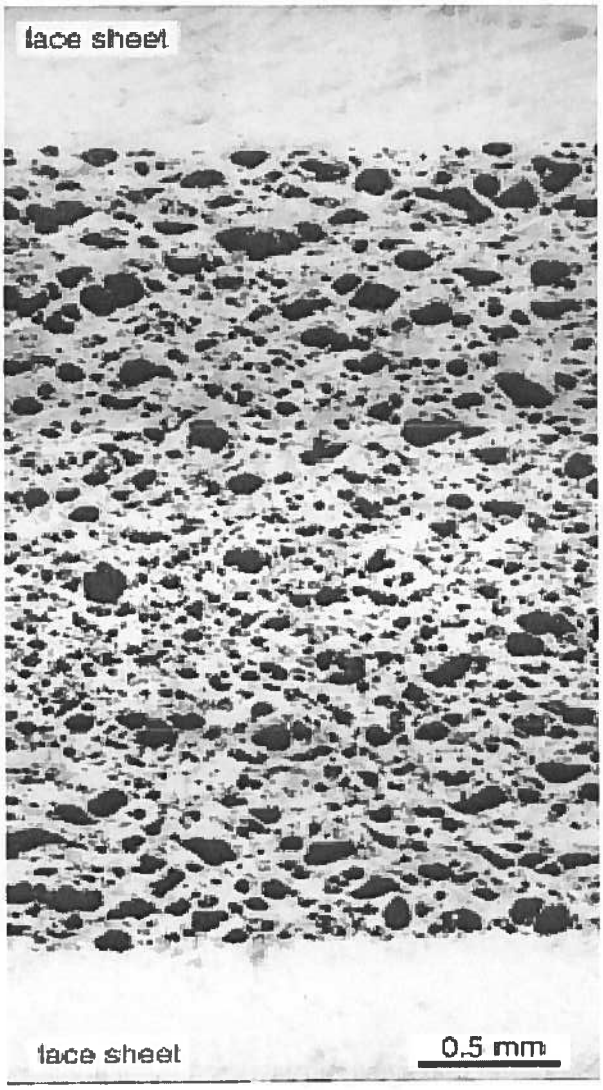

Fig. 7 Ti-6Al-4V sandwich structure with a porous core (courtesy, Schwartz et al. [112]).

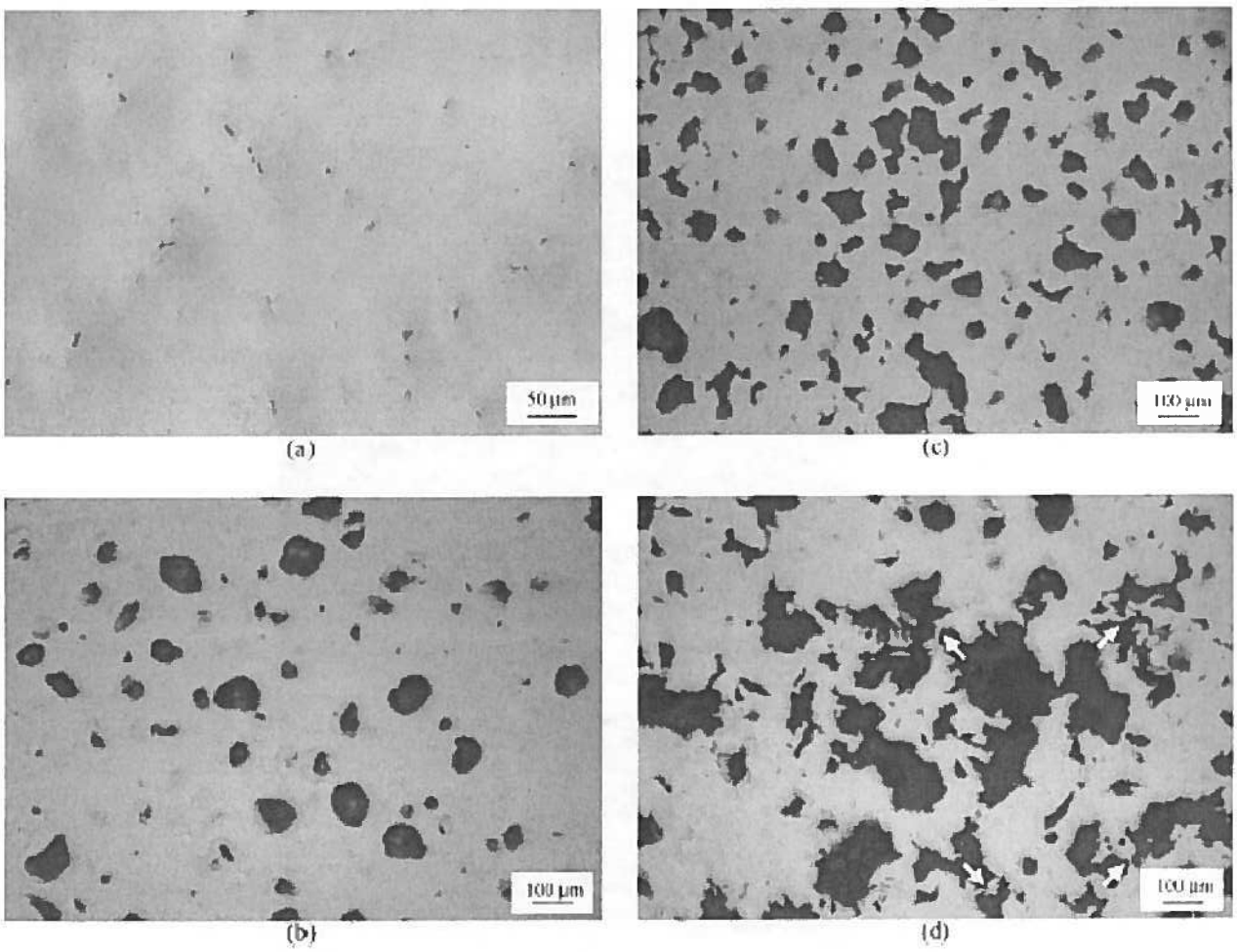

Fig. 8 Microstructure evolution during superplastic entrapped gas expansion of CP-Ti (a) 0 h, (b) 8 h, (c) 26 h, (d) 83 h (courtesy, Murray et al. [115]).

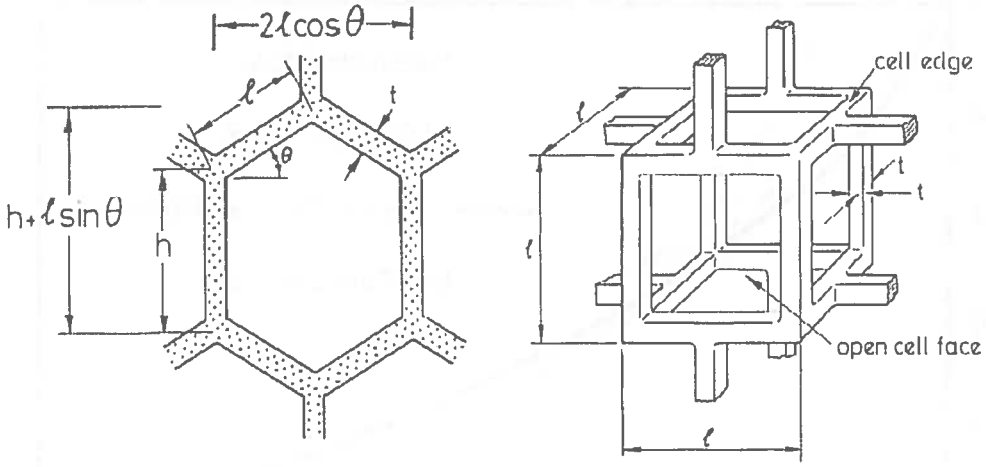

Fig. 9 The unit cells used by Gibson and Ashby to model the foam and cellular materials[44] (a) 2D hexagonal honeycomb cell, (b) 3D cubic open cell.

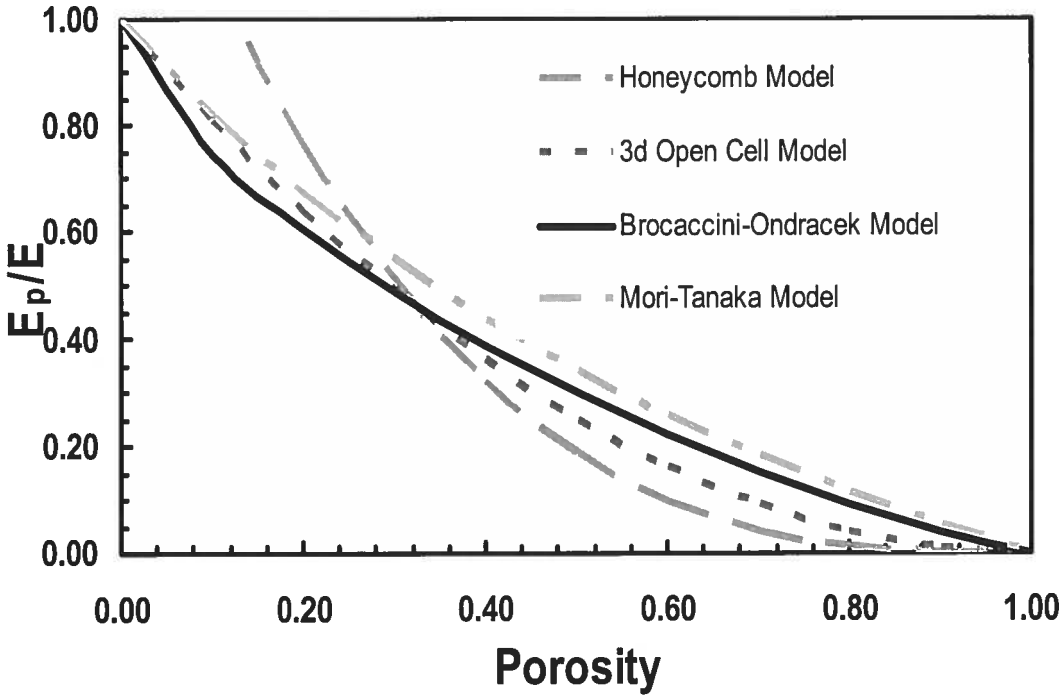

Fig. 10 Theoretical predictions for the Young's modulus using the various models

Table 1: Comparison of mechanical properties of typical metallic and ceramic biomaterials with human bones. [6]

Material	Young's Modulus (GPa)	Tensile strength (MPa)
Metal and alloy		
Stainless steel	190	586
Co-Cr alloy	210	1085
Ti-alloy	116	965
Ti	110	550
Amalgam	30	58
Ceramics		
Alumina	380	300
Zirconia	220	820
Bioglass	35	42
Hydroxyapatite (HA)	95	50
Cortical bone	7-30	50-150

Table 2: Summary of processing and mechanical results for porous titanium and its alloy compacts by powder sintering.

Researchers/ Authors	Initial powder	Main processing Parameters	Porosity	Mechanical Properties	Ref.
Cirincione et al.	Ti-6Al-4V	Loose powder sintering at 1000°C, 0.5-24h	41-55%	Maximum compressive strength: 55MPa for 49% porosity	[85]
Oh, et al.	Spherical Ti (65μm, 189μm and 374μm)	Compacting pressure: 70MPa for 10 min. sintering at 900/1100/1300°C, 2hrs, sintering pressure: 0/5/10 MPa	5-37%	Modulus: 10-90GPa Bending Strength: 100-750MPa. Both modulus and strength decrease linearly with increasing porosity.	[87-88]
Kon et al.	Spherical Ti (80 μm) Spherical Ti-6Al-4V (76 μm)	Electro-discharge compaction Sintering temperature (600-700°C), time: 3-20 mins Sintering pressure: 20-30MPa,	~30%	Bending strength: 128-178MPa Elastic modulus: 16-18GPa	[93]
Thieme et al.	Ti (180-1000 μm)	Sintering temperature: 1150/1370/ 1470°C sintering time: 1-3 hrs	35-60%	Modulus: 5-35 GPa, Bending strength: 26-184 MPa	[89]

Table 3: Summary of processing and mechanical results for porous titanium and its alloy compacts by using space holder or pore-forming agents.

Researchers/ Authors	Space-holder or Pore-forming agents	Sintering Parameters	Porosity	Mechanical Properties	Ref.
Wheeler et al.	Mg powder/wires evaporated at 1000°C	1400°C	25-82%	Strength: 15-607MPa Modulus: 3-9GPa	[96]
Bram et al.	Carbamide $(NH_2)_2CO$ and ammonium hydrogen carbonate $(NH_4)HCO_3$ Completely removed under 200°C	1400°Cx1h	60%,77% pore size 0.1-2.4 mm	Compressive plateau stress :10 MPa and 100MPa for 77% and 60% porosity, respectively Bending strength: 5.6MPa for 77% 68MPa for 60%	[98]
Wen et al.	Ammonium hydrogen carbonate $(NH_4)HCO_3 \rightarrow NH_3+CO_2+H_2O$ removable at 200°Cx5h	1200°Cx2h	35-80%	Compressive strength: 25-748MPa. Young's Modulus: 2.9-10.3 GPa	[100]
Rausch et al.	Polymer granules that can be chemically removed at 130°C	1100-1250°C	55-80%	Tensile strength: 1.5-30MPa Young's modulus: 0.3-16GPa	[97]
Gauthier et al.	Polymeric binder plus foaming agent	(1) Foaming (2) Debinding (3) sintering	66-79%	Compressive yield stress: 10-22MPa Modulus: 0.6-2.1GPa	[106]

Table 4: Summary of processing and mechanical results for porous titanium and its alloy compacts by entrapped gas expansion.

Researchers/ Authors	Processing Parameters	Porosity	Mechanical Properties	Ref.
Davis et al.	(1) Powders packing in vacuum and backfilled with Ar pressure of 3.3 atm. (2) Densification by HIP at 890°C at 100MPa for 125 min. (3) Foaming at creeping temperature (isothermal) of 903/960°C or at superplastic thermal cycling of 830-980°C for 1-24 h for gas expansion	22-27% isothermal foaming 41% thermal cycling foaming.	Compressive yield strength of 200MPa and Young's modulus of 60GPa are observed for 22% sample Compressive yield strength of 120MPa and Young's modulus of 39GPa were observed for 41% sample.	[114]